Biophysical Chemistry, 32 (1988) 297–303
Elsevier

BPC 01334

Conformational dynamics of cytochalasin B in solution as detected by ^{13}C and ^{1}H NMR relaxation rates

E. Gaggelli [a], A. Maccotta [b], A. Scopa [b] and G. Valensin [b]

[a] *Department of Chemistry, University of Siena, 53100 Siena and* [b] *Institute of Chemistry, University of Basilicata, 85100 Potenza, Italy*

Received 3 August 1988
Accepted 24 October 1988

Cytochalasin; ^{13}C-NMR; ^{1}H-NMR; Spin-lattice relaxation rate

^{13}C and ^{1}H NMR spin-lattice relaxation rates have been measured for cytochalasin B in $[^{2}H]_6$DMSO. Motional features have been interpreted in terms of nearly isotropic reorientation of the whole molecule with few additional internal motions. The 'isotropic' reorientational correlation time was evaluated at 0.21 ns at room temperature. By using selective and double-selective excitation techniques, relevant cross-relaxation terms have been obtained wherefrom proton–proton distances have been calculated. A Dreiding model of the 'preferred' conformation in solution has been built, yielding evidence of a strong similarity between solution and solid state structures of cytochalasin B.

1. Introduction

The cytochalasins are a group of fungal metabolites that interfere with many cellular motile functions such as endocytosis, cell movement, and pseudopod extension and retraction [1]. Cytochalasin B (CB) (fig. 1) has been shown to tightly bind to the growing ends of actin filaments, thus blocking further elongation [2–4]. Moreover, CB is a very specific and potent inhibitor of D-glucose transport in human erythrocytes [5,6] and this property has been used to identify the glucose transporter in plasma and microsomal membranes [7].

On the basis of details of solid state structures [8], a model was proposed for cytochalasin interacting with the glucose carrier through hydrogen bonds at N_2, O_7 and O_{23}. In such a model, the hydrophobic region from C_{13} to C_{19} was suggested to act as an anchor in some hydrophobic domain of the glucose carrier [9].

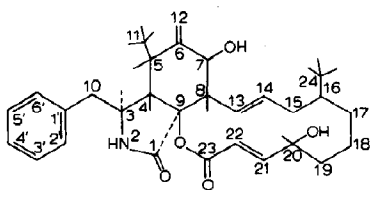

Fig. 1. Molecular formula of cytochalasin B.

^{1}H NMR studies on CB in solution [10] provided evidence of a preferred conformation, as determined by 1D and 2D magnetization transfer experiments, very close to the solid state structure of cytochalasin A [6] and the two macrocyclic ligands were assumed to be of very similar conformation in solution.

In this communication ^{13}C- and ^{1}H-NMR relaxation studies at two frequencies have been utilized in the evaluation of motional features and intramolecular internuclear distances within the CB molecule in solution of $[^{2}H]_6$DMSO. ^{13}C-^{1}H and ^{1}H-^{1}H dipole–dipole interaction energies between well defined spin pairs have been evaluated by measuring selective and double-selective proton spin-lattice relaxation rates. Selective pulse techniques are, in fact, well known to provide a means of isolating the dipolar term of any single proton pair from the broad envelope of mutual pairwise interactions [11–14].

Information gained from relaxation rates, together with that from J coupling constants and from the temperature dependence of chemical shifts, were utilized in the construction of a Dreiding model of the 'preferred' conformation in solution.

2. Material and methods

Cytochalasin B supplied by Sigma Chemical Co. was used without further purification. Solutions were made in $[^2H]_6$DMSO 99.96% (Merck) and were carefully deoxygenated by bubbling nitrogen gas. The NMR experiments were carried out on a Varian VXR-200 and on a Bruker AM-300 FT-NMR spectrometer at probe temperatures of $25 \pm 1°C$. Chemical shifts were referenced to internal $[^2H]_4$TSP 2 mmol dm^{-3}. Assignments were done by obtaining homo- and hetero-nuclear shift correlated 2D NMR spectra and by comparison with literature data.

^{13}C and ^{1}H nonselective spin-lattice relaxation rates were measured with the inversion recovery pulse sequence $(t\text{-}180\text{-}\tau\text{-}90)_n$. 80 and 12 FIDs were respectively collected for each experiment and the relaxation rates were calculated with an exponential regression analysis of the recovery curves of longitudinal magnetization components by using the computer of the spectrometer.

Selective and double-selective proton spin-lattice relaxation rates were measured with inversion recovery pulse sequences in which the 180° pulse was provided by the proton decoupler switched on for relatively long times at the selected frequencies at low power. Typical experimental settings for a 180° pulse were 20–30 ms with 12–18 db attenuation. The 90° pulse was, in contrast, the usual nonselective 90° pulse provided by the proton transmitter. The corresponding relaxation rates were calculated in the initial rate approximation [15]. Magnetization transfer 2D ^{1}H NMR experiments were performed using the pulse sequence described in ref. 16 with mixing times from 0.1 to 0.5 s. The spectral width was 2000 Hz, and the data set consisted of 1024 points in both the t_1 and t_2 dimensions. 16 FIDs were collected for each value of t_1 for a total accumulation time of ~ 8 h.

3. Results and discussion

The ^{13}C-{^{1}H} NOEs of all protonated carbons were found at their maximum values, thus demonstrating that the ^{13}C-^{1}H dipolar interaction provides the most relevant relaxation mechanism for ^{13}C nuclei. Information on molecular motions can be therefore obtained from ^{13}C spin-lattice relaxation rates normalized for the number of attached protons (R_1/n_H) [17]. R_1 and R_1/n_H values are reported in table 1 together with chemical shifts. It is evident that, with the exception of methyls, all carbons are characterized by relatively fast relaxation rates not very different from each other.

Table 1

75.14 MHz ^{13}C NMR parameters of CB 0.05 mol dm^{-3} in $[^2H]_6$DMSO ($T = 298$ K)

Carbon	δ (ppm)	R_1 (s^{-1})	R_1/n_H (s^{-1})
C_1	170.69	0.32 ± 0.01	–
C_{23}	164.10	0.40 ± 0.01	–
C_{21}	153.31	5.26 ± 0.62	5.26
C_6	150.95	0.86 ± 0.02	–
$C_{1'}$	137.03	0.58 ± 0.01	–
C_{14}	133.15	4.17 ± 0.37	4.17
$C_{2',6'}$	129.67	3.45 ± 0.12	3.45
C_{13}	128.52	4.76 ± 0.79	4.76
$C_{3',5'}$	128.24	3.45 ± 0.12	3.45
$C_{4'}$	126.39	4.17 ± 0.59	4.17
C_{22}	118.09	4.45 ± 0.41	4.45
C_{12}	112.31	11.11 ± 0.98	5.55
C_9	83.33	0.25 ± 0.01	–
C_7	69.43	3.70 ± 0.41	3.70
C_{20}	68.58	4.17 ± 0.59	4.17
C_3	52.34	3.33 ± 0.62	3.33
C_8	47.50	4.35 ± 0.52	4.35
C_4	46.52	5.26 ± 0.57	5.26
C_{10}	42.87	6.25 ± 0.64	3.12
C_{19}	41.67	7.69 ± 0.81	3.85
C_{15}	34.39	6.67 ± 0.70	3.33
C_{18}	34.36	12.50 ± 1.04	6.25
C_{16}	32.91	4.76 ± 0.42	4.76
C_5	31.00	5.00 ± 0.39	5.00
CH_3 (24)	20.31	2.32 ± 0.26	0.77
C_{17}	20.03	6.67 ± 0.71	3.33
CH_3 (11)	13.23	4.17 ± 0.39	1.39

Table 2

200 and 300 MHz ^{1}H-NMR chemical shifts, nonselective (R^{nsel}) and selective (R^{sel}) spin-lattice relaxation rates and F ratios ($F = R^{nsel}/R^{sel}$) for CB 0.05 mol dm^{-3} in [^{2}H]$_6$DMSO ($T = 298$ K)

Proton	δ (ppm)	$\nu = 200$ MHz			$\nu = 300$ MHz		
		R^{nsel} (s^{-1})	R^{sel} (s^{-1})	F	R^{nsel} (s^{-1})	R^{sel} (s^{-1})	F
H_{17a}	0.71	8.00			9.09		
CH_3 (11)	0.81	5.88	5.95	0.99	5.26		
CH_3 (24)	1.01	4.03			5.26		
H_{16}	1.30	5.78			4.17		
H_{18e}	1.47	8.20			6.67		
H_{18a}	1.54	8.62			6.26		
H_{19e}	1.64	7.87			6.25		
H_{15a}	1.69	8.55			7.14		
H_{17e}	1.86	8.33					
H_{19a}	2.07	7.46	5.78	1.29	6.06		
H_{10}	2.63	3.42					
H_4	2.73	6.90					
H_5	2.94	4.41	3.48	1.27			
H_8	3.09	4.08					
H_3	3.14	6.21					
H_7	3.48	2.26	1.94	1.16	1.05		
H_{20}	4.15	3.27	2.67	1.22	2.50		
OH (7)	4.53	1.57	1.68	0.93	1.04		
$H_{12'}$	4.62	5.68	4.20	1.35	4.00	3.12	1.28
OH (20)	4.71	1.88					
H_{14}	4.77	1.76					
$H_{12''}$	4.82	4.74	3.62	1.31	3.23		
H_{22}	5.34	1.19	1.01	1.18	0.86		
H_{13}	5.44	2.10			1.12		
H_{21}	6.28	2.69	2.35	1.14	2.03	1.69	1.20
$H_{2',6'}$	6.58	1.81				1.27	
$H_{4'}$	6.66	1.32					
$H_{3',5'}$	6.73	1.33					
NH	7.61	3.36	3.12	1.08	2.74	2.56	1.07

If one considers that (i) the slowest and the fastest relaxation rates would yield, according to eq. 2, quite similar values for the motional correlation time (0.15 and 0.31 ns respectively) and also that (ii) the CB molecule is not likely to have several degrees of freedom, isotropic or nearly isotropic reorientational motions can be assumed as the simplest framework for interpretation of spin-lattice relaxation rates. As a consequence, a correlation time of 0.21 ns was taken for isotropic reorientation of CB in solution at room temperature. The choice of an 'isotropic' correlation time was supported by the following properties of ^{1}H NMR spin-lattice relaxation rates:

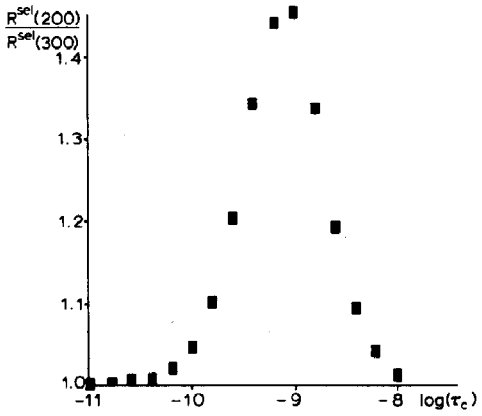

Fig. 2. Theoretical plot of $R^{sel}(200)/R^{sel}(300)$ as a function of the motional correlation time.

Table 3

Cross-relaxation rates between proton pairs of CB 0.05 mol/dm^3 in [^{2}H]$_6$DMSO (T = 298 K)

Proton pair	σ_{ij} (s^{-1})
H_3-NH (2)	0.19
H_7-OH (7)	0.32
H_5-CH_3 (11)	0.16
$H_{12'}$-$H_{12''}$	1.16
H_{19a}-H_{20}	0.04
H_{20}-H_{21}	0.05
H_{21}-H_{22}	0.06

(a) The selective rates of some protons (table 2), are frequency dependent, suggesting that the motional correlation time is outside the extreme narrowing region [18]. The ratio $R^{sel}(200)/R^{sel}(300)$ provides a means of calculating τ_c, as shown in fig. 2. From such ratios $\tau_c = 0.30 \pm 0.05$ ns was evaluated in a very good agreement with the τ_c calculated from ^{13}C relaxation rates.

(b) Some protons of CB are found at fixed distances and can be therefore taken as the target of double-selective irradiation experiments in order to calculate τ_c. The difference between the double-selective and the selective spin-lattice relaxation rates can be in fact shown to yield the cross-relaxation rate between the two irradiated protons [11–14]. All the calculated cross-relaxation rates σ_{ij} are reported in table 3. Among them, $\sigma_{12',12''}$ and $\sigma_{3,NH}$ can be suitably considered for evaluation of the motional correlation time since $r_{12',12''}$ and $r_{3,NH}$ can be easily obtained from the Dreiding model of the CB molecule. $\tau_c = 0.18$ ns and $\tau_c = 0.23$ ns were calculated from the cross-relaxation terms between the $H_{12'}$ and $H_{12''}$ protons and between the H_3 and NH protons respectively.

(c) The cross-relaxation rate of H_5, as measured by double-selective irradiation of the AX_3 spin system H_5-CH_3(11), table 3, can be approximated by considering that the A proton always experiences dipolar interactions with any two gauche X_3 protons. This would lead to a value of 0.07 ns for the effective correlation time modulating such dipolar interactions. Such effective correlation time is consistent with rapid internal motion of the methyl group around the C_5-C_{11} axis that reorients with a correlation time of 0.25 ns [18].

It can be concluded that molecular dynamics are consistently approximated by isotropic or nearly isotropic motion of the whole molecule with some degrees of freedom for internal rotation of the methyl groups and for libration of the aromatic ring around the $C_{1'}$-$C_{4'}$ axis. It can be in fact noticed that $C_{4'}$ relaxes with a relatively faster rate than the other aromatic protonated carbons. By applying the model of Woessner [19] for a C-H vector undergoing internal motion around an axis reorienting isotropically and making an angle of 60° with the vector, the correlation time for librational motion can be calculated at 0.07 ns.

By assuming the previous dynamic picture, expected values for direct- and cross-relaxation terms can be calculated for different kinds of proton pairs, as shown in table 4. By considering the proton relaxation rates (tables 2 and 3) several conformational features can then be obtained.

The cross-relaxation term $\sigma_{19a,20}$ (table 3) is typical of two vicinal *trans* protons, thus suggesting that H_{20} is in axial position; whereas the cross-relaxation term $\sigma_{20,21}$ allows to locate the H_{21} at 2.8 Å from H_{20}, that is to say in a gauche or nearly gauche position. Since H_{21} and H_{22} are in *trans* with respect to each other, as also verified by the corresponding cross-relaxation term, it is possible to delineate that H_{21} is in an inward equatorial position while H_{22} is outward equatorial. Moreover, if one considers that the overall cross-relaxation rate of H_{22}, as measured by the

Table 4

Calculated direct- and cross-relaxation terms for some proton spin pairs in a molecule undergoing isotropic motion with a reorientational correlation time of 0.21 ns

Spin pair	Distance (Å)	ν = 200 MHz		ν = 300 MHz	
		ρ_{ij} (s^{-1})	σ_{ij} (s^{-1})	ρ_{ij} (s^{-1})	σ_{ij} (s^{-1})
Geminal sp^3	1.77	3.30	1.43	2.83	1.04
Geminal sp^2	1.84	2.62	1.14	2.24	0.83
Vicinal aromatic	2.43 [a]	0.49	0.21	0.42	0.16
Vicinal *gauche*	2.47	0.45	0.19	0.38	0.14
Vicinal *trans*	3.07	0.12	0.05	0.10	0.04

[a] From neutron scattering data (ref. 21).

difference $R_{22}^{nsel} - R_{22}^{sel}$, is much faster than the cross relaxation term $\sigma_{21,22}$ (table 3), the dipolar interaction with the hydroxyl proton OH(20) has to be taken into account, yielding a distance of 2.7 Å between the two protons. Such distance is consistent with a gauche arrangement, either g^+ or g^-, of the two protons around the C-O bond. These findings are ratified by the overall cross-relaxation rate of H_{20} ($\Sigma\sigma_{ij} = R_{20}^{nsel} - R_{20}^{sel}$) that can be fitted with three gauche and one *trans* contributions. On the contrary, in order to account for the overall cross-relaxation rate of H_{21}, the dipolar interaction with H_{17e} must be considered, as strongly suggested by the nuclear Overhauser effect between the two measured in 1D and 2D experiments in the present as well as in previous works [10]. The following relationship can be written:

$$\sum_{j \neq 21} \sigma_{21,j} = \sigma_{21,22} + \sigma_{21,20} + \sigma_{21,17e} \qquad (1)$$

wherefrom the cross-relaxation term $\sigma_{21,17e} = 0.23$ s^{-1} can be obtained, yielding 2.4 Å for the corresponding internuclear distance.

The last measured cross-relaxatin rate between H_7 and the attached hydroxyl proton (0.32 s^{-1}) suggests that the two protons are 2.3 Å apart in a gauche or nearly gauche arrangement. It is worth noting that all these features lead to the conclusion that the lone pairs of both hydroxyl oxygens are in appropriate position to build up hydrogen bonding networks with the solvent, as also demonstrated by the temperature dependence of chemical shifts of exchangeable protons. The large values of the temperature coefficients (0.008–0.010 ppm/°C) were in fact consistent with the occurrence of freely solvated groups [20].

The two geminal $H_{12'}$ and $H_{12''}$ protons have quite different spin-lattice relaxation rates, either nonselective or selective. This property can only be explained by assuming that one or more dipole–dipole interactions are contributing to the relaxation pathway of only one of the two protons. As a matter of fact, if the difference between nonselective and selective relaxation rates is considered ($R^{nsel} - R^{sel} = \Sigma_{i \neq j}\sigma_{ij}$), the cross-relaxation term $\sigma_{12'12''}$ (table 3) accounts completely for the observed difference in one case, while a residual cross-relaxation rate of 0.34 s^{-1} is contributing in the other case. If H_5 and H_7 were both dipolarly coupled with H_{12} protons, no difference should have been found in the relaxation rates; moreover, if H_7, and not H_5, were affecting relaxation of one of the H_{12} protons, a certain dipolar contribution to methyl protons should have been measured; as a consequence, it can be concluded that H_5, and not H_7, is contributing to relaxation of the H_{12} proton at low field. This being the case, H_5 must be equatorial, whereas H_7 has to be axial. In such an arrangement a distance of 2.3 Å is measured between H_5 and H_{12} in the Dreiding model, yielding a cross-relaxation term of 0.30 s^{-1}.

The sum of cross-relaxation terms contributing to the cross-relaxation rate of the NH proton (0.24 s^{-1} at 200 MHz and 0.18 s^{-1} at 300 MHz, as inferred by the differences $R_{NH}^{nsel} - R_{NH}^{sel}$) is completely accounted for by considering the NH-H_3 and the NH-H_{10} dipolar interactions. The former spin pair is at a fixed distance and yields $\sigma_{NH,H_3} = 0.19$ s^{-1}; whereas the second spin pair provides a cross-relaxation term of 0.07 s^{-1} by measuring the distance between the equatorial H_{10} proton and the NH in the Dreiding model. The same set of values ($r_{NH,H_3} = 2.5$ Å, $r_{NH,H_{10}e} = 2.9$ Å, $\tau_c = 0.21$ ns) accounts for the observed cross-relaxation rate at 300 MHz. It follows that there are not other protons close enough to the NH, thus excluding the possibility of certain orientations of the aromatic ring. Moreover, the relaxation rates of aromatic protons disclose the striking feature that the ortho hydrogens, in spite of an apparently poorer dipolar environment, possess the fastest nonselective rates. Taking the interaction between H_{10} and ortho protons into account leads to the conclusion that the plane of the ring is very likely to be almost perpendicular to the axis of the C_3-C_{10} bond, but still does not completely explain the very fast relaxation rate. The only possibility is a certain dipolar interaction with CH_3(11) methyl protons: an internuclear distance of 2.2 Å, modulated by the correlation time for internal motions would yield, in fact, a contribution of 0.51 s^{-1} to the nonselective spin-lattice relaxation rate of ortho protons, that, summed up with the contributions of meta and H_{10} protons, would provide a good fitting of the observed value.

As a final step in conformational analysis of cytochalasin B in solution, fitting the nonselective relaxation rates of H_{13} and H_{14} was attempted. The splitting pattern of such resonances, in fact, did not allow to reach suitable conditions for selective irradiation. Fitting a nonselective relaxation rate is likely to be a much more approximate trial than interpreting a cross-relaxation rate, especially because it is not possible to get rid of eventual contributions from 'other' relaxation mechanisms. Anyway it came out that only one possible spatial arrangement could provide a suitable framework for obtaining good approximations of the experimental relaxation rates. In such an arrangement both H_{13} and H_{14} are axial, upward and downward respectively. H_{13} is dipolarly coupled with H_{14} ($r = 3.1$ Å, $R^{nsel} = 0.18\ s^{-1}$), H_7 ($r = 2.6$ Å, $R^{nsel} = 0.47\ s^{-1}$), H_8 ($r = 3.1$ Å, $R^{nsel} = 0.18\ s^{-1}$), OH(7) ($r = 2.8$ Å, $R^{nsel} = 0.29\ s^{-1}$) and H_{15a} ($r = 2.3$ Å, $R^{nsel} = 0.98\ s^{-1}$); whereas H_{14} experiences dipolar contributions from H_{13} ($r = 3.1$ Å, $r^{nsel} = 0.18\ s^{-1}$), H_{15e} ($r = 2.5$ Å, $R^{nsel} = 0.65\ s^{-1}$).

All the evaluated conformational features were in reasonable agreement with coupling constants reported in a previous work [10] and allowed us to build up a model of the most probable spatial arrangement in solution. This is shown in fig. 3 as a perspective view obtained with the help of the molecular graphics package implemented on a Vax 750 computer connected to a digital VT 240 graphics terminal [22]. The agreement with the solid state structure [8,9] is quite good. Crystallographic determinations were in fact pointing to (a) distorted boat conformation of the six-membered ring; (b) planar conformation of the five-membered ring; (c) g^- conformation of the point of attachment of the phenyl ring around the C_3-C_{10} bond; (d) flatness of the C_{20}-C_{23} portion; (e) parallelism between the phenyl ring and the macrocycle.

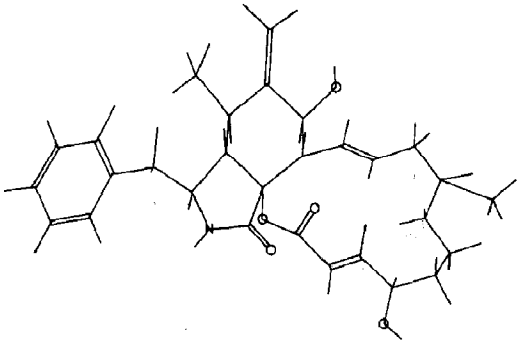

Fig. 3. Perspective view of the 'preferred' conformation of CB in DMSO solution (see text for details).

The fact that the preferred conformation in solution agrees with the solid state structure is very likely to ratify the model for the inhibition of glucose transport by CB. Such a model has in fact been suggested on the basis of the solid state structures of β-D-glucose and eight cytochalasin molecules [9].

References

1 S.W. Tannebaum, Cytochalasins: biochemical and cell biological aspects (Elsevier, Amsterdam, 1978).
2 D.C. Lin and S. Lin, Proc. Natl. Acad. Sci. USA 76 (1979) 2345.
3 M. Grumet and S. Lin, Biochem. Biophys. Res. Commun. 92 (1980) 1327.
4 M.D. Flanagan and S. Lin, J. Biol. Chem. 255 (1980) 835.
5 C.Y. Jung and A.L. Rampal, J. Biol. Chem. 252 (1977) 5456.
6 A.L. Rampal, H.B. Pinkofsky and C.Y. Jung, Biochemistry 19 (1980) 679.
7 L.J. Wardzala and B. Jeanrenaud, Biochim. Biophys. Acta 730 (1983) 49.
8 G.M. McLaughlin, G.A. Sim, J.R. Kiechel and C. Tamm, Chem. Commun. (1970) 1398.
9 J.F. Griffin, A.L. Rampal and C.Y. Jung, Proc. Natl. Acad. Sci. USA 79 (1982) 3759.
10 D.W. Graden and D.G. Lynn, J. Am. Chem. Soc. 106 (1984) 1119.
11 L.D. Hall and H.D.W. Hill, J. Am. Chem. Soc. 98 (1976) 1269.
12 N. Niccolai, M.P. Miles, S.P. Hehir and W.A. Gibbons, J. Am. Chem. Soc. 100 (1978) 6528.
13 G. Valensin, G. Sabatini and E. Tiezzi, in: Advanced magnetic resonance techniques in systems of high molecular complexity, eds. N. Niccolai and G. Valensin (Birkhauser, Boston, 1986) p. 69.
14 E. Gaggelli, N. Marchettini and G. Valensin, J. Chem. Soc., Perkin Trans. II (1987) 1707.
15 R. Freeman, H.D.W. Hill, B.L. Tomlinson and L.D. Hall, J. Chem. Phys. 61 (1974) 4466.
16 A. Kumar, R.R. Ernst and K. Wüthrich, Biochem. Biophys. Res. Commun. 95 (1980) 1.

17 A. Allerhand, D. Doddrell and R. Komoroski, J. Chem. Phys. 55 (1971) 189.
18 J.H. Noggle and R.E. Schirmer, The nuclear Overhauser effect (Academic Press, New York, 1971).
19 D.E. Woessner, J. Chem. Phys. 36 (1962) 1.
20 M. Ohnishi and D.W. Urry, Biochem. Biophys. Res. Commun. 36 (1969) 194.
21 M.N. Frey, T.F. Koetzle, M.S. Lehmann and W.C. Hamilton, J. Chem. Phys. 58 (1973) 2547.
22 C. Still, 'Macromodel', Columbia University Molecular Modeling System, 1987.